Directional Grouping of Decaying Modes in a Reverberation Room

Marco Berzborn and Michael Vorländer
Institute of Technical Acoustics, RWTH Aachen University, 52074 Aachen, Germany
Email: marco.berzborn@akustik.rwth-aachen.de

Introduction

The random-incidence absorption coefficient is measured in a reverberation room based on Sabine's theory with the underlying assumptions of an isotropic and homogeneous sound field as well as a uniform damping of the modes constituting the latter. Both assumptions are violated in standardized absorption coefficient measurements, at the latest when an absorbing sample is placed in the room [1, 2]. The consequence is a poor reproducibility across different laboratories [3]. Based on an analytic model for rectangular rooms Hunt et al. [1] showed that axial, tangential, and oblique modes inherit different damping constants, even for uniform distributions of boundary conditions. They further showed that a different boundary condition on a single different room surface results in distinct multi-exponential decay curves due to non uniform damping of modes. More recently, based on a statistical energy model, Nilsson [4] showed that the resulting energy decay curve (EDC) in a room with absorption concentrated on a single surface is governed by two main decay constants. This was also found by Balint et al. [5] who used a Bayesian approach to estimate the decay constants from EDCs measured in a reverberation room. However both methods lack spatial information about the damping of modes.

In [6, 7] the authors presented the directional energy decay curve (DEDC) – calculated as the Schroeder integral evaluated on a sound field decomposed into its angular wavenumber spectrum – for the analysis of sound field isotopy during the decay process, giving insights into the angular distribution of the remaining energy in the decaying sound field. This contribution aims at analyzing the angular distribution of average decay times of modes grouped according to their direction of arrival (DOA) in the angular wavenumber spectrum. The average decay times for each group are estimated from the DEDC for the corresponding direction.

The first section briefly introduces the concept and calculation of the DEDC and the required array signal processing framework for the sound field decomposition. the second section introduces the experimental setup in a reverberation room occupied with an absorber and with and without panel diffusers. The results and conclusions are presented in the last two sections of this paper.

Directional Energy Decay Curves

Spherical microphone arrays (SMAs) allow for the capture of directional room impulse responses (DRIRs) retaining angular information about the sound field in the room [8]. A DRIR measured with an SMA can be written as a vector of L microphone signals

$$\mathbf{p}(k) = \left[p(k, r, \theta_1, \phi_1), \ldots, p(k, r, \theta_L, \phi_L)\right]^{\mathrm{T}}, \quad (1)$$

where θ_l and ϕ_l are the elevation and azimuth angles of the l'th sensor position, respectively, k is the wave number, and $(.)^{\mathrm{T}}$ denotes the transpose operator. For a plane wave sound field we may write the sound pressure at the microphone positions of an SMA as [9]

$$\mathbf{p}(k) = \mathbf{B}(k)\mathbf{a_{nm}}(k), \quad (2)$$

where the matrix $\mathbf{B}(k)$ contains the spherical harmonic (SH) basis functions[1] $Y_n^m(\theta_l, \phi_l)$ of order n and degree m evaluated at the elevation and azimuth angles, as well as the modal strength function for the sphere, both with a maximum SH order N. The vector $\mathbf{a_{nm}}(\mathbf{k})$ contains the SH coefficients defining the amplitude density function of the plane waves composing the sound field. For a single plane wave incident this becomes a vector containing the SH basis functions evaluated at the DOA. Solving Eq. (2) for the spatial domain plane wave density function $\mathbf{a}(k)$ we decompose the sound field into a continuum of Q plane waves [10]

$$\mathbf{a}(k) = \mathbf{Y}\mathbf{W_{nm}}\mathbf{B}^{\dagger}(k)\mathbf{p}(k), \quad (3)$$

where the $(.)^{\dagger}$ operator denotes the Moore-Penrose Pseudo-inverse and

$$\mathbf{Y} = \left[\mathbf{y}^{\mathrm{T}}(\theta_1, \phi_1), \ldots, \mathbf{y}^{\mathrm{T}}(\theta_Q, \phi_Q)\right]^{\mathrm{T}}, \quad (4)$$

is the steering matrix of the array containing vectors of the SH basis functions evaluated at the q'th steering direction

$$\mathbf{y}(\theta_q, \phi_q) = \left[Y_0^0(\theta_q, \phi_q), \ldots, Y_N^N(\theta_q, \phi_q)\right], \quad (5)$$

and $\mathbf{W_{nm}}$ is a diagonal matrix containing Dolph-Chebyshev weights [10] for uniform side-lobe attenuation. The plane wave density function $\mathbf{a}(k)$ is also referred to as the two-dimensional angular wave number spectrum spanned over the spherical domain (θ, ϕ) [11]. Here, it is interpreted as a two-dimensional projection of the three-dimensional wave number spectrum of the modes in a room as defined in [1] for a single point in the room. Given that the modes are not degenerate we assume that groups of axial, tangential and oblique modes are represented as a corresponding sum of plane waves in the angular wave number spectrum. As an example, the group of axial modes in the x-axis of a rectangular room corresponds to a sum of two plane waves traveling in $+x$ and $-x$ directions, respectively. It has to be noted that

[1] We use real valued SH basis functions following the Ambix phase convention and N3D normalization.

this grouping does not allow for a separation of modes in a strict sense, as already all aforementioned axial modes share the same DOAs.
In [6, 7] the authors proposed the DEDCs as the Schroeder integral [12] of the inversely Fourier transformed angular wave number spectrum (cf. Eq. (3)), yielding the DEDCs for every steering direction

$$\mathbf{d}(t) = \int_t^\infty |\mathbf{a}(\tau)|^2 d\tau \quad = \mathbf{e_s} - \int_0^t |\mathbf{a}(\tau)|^2 d\tau, \qquad (6)$$

where $\mathbf{e_s}$ is a vector containing the steady state energy for every steering direction. Here, it may be interpreted as the decay curve for a group of modes corresponding to the respective DOA defined by (θ_q, ϕ_q). Assuming that the modes in every group follow a joint average damping constant $\langle\gamma(\theta_q, \phi_q)\rangle$, we may calculate a corresponding mean decay time $\langle T(\theta_q, \phi_q)\rangle$ for every group.

Experimental Setup

The DEDCs were analyzed experimentally for a rectangular reverberation room at the Technical University of Denmark (2800 Kgs. Lyngby, Denmark) in two configurations[2]: With and without panel diffusers, in both cases occupied with an absorbing sample of glass wool with a flow resistivity of $12.9\,\mathrm{kPa \cdot s/m^2}$, a thickness of 100 mm, and a surface area of $10.8\,\mathrm{m^2}$. The dimensions of the room are $(x, y, z) = (6.25\,\mathrm{m}, 7.85\,\mathrm{m}, 4.9\,\mathrm{m})$ with an approximate volume of $245\,\mathrm{m^3}$ and a Schroeder frequency slightly over 300 Hz. A sequential dual-layer SMA centered at $(2.98\,\mathrm{m}, 4.16\,\mathrm{m}, 1\,\mathrm{m})$ (cf. Fig. 1) was sampled using a UR5 (Universal Robots, Odense, Denmark) scanning robot arm moving a pressure-field 1/2″ Brüel & Kjær type 4192 microphone. The SMA consists of 144 sampling positions distributed according to a equal-area partitioning [14] of the two spheres with radii $r = (0.25\,\mathrm{m},\ 0.45\,\mathrm{m})$. The eigenfrequencies of the spheres were additionally stabilized by sampling points inside each sphere [15]. Impulse response measurements were performed with the ITA-Toolbox [16] using exponential sweeps driving a source mounted in the corner below the ceiling at approximately $(0.2\,\mathrm{m}, 0.2\,\mathrm{m}, 4.7\,\mathrm{m})$. The duration for sampling a full sequential array required 2.5 h. Temperature changes remained below 0.3 °C during the procedure.
The estimation of the angular wavenumber spectrum was performed for a SH order $N = 7$ for 1026 steering directions on an equi-angular grid. The Dolph-Chebyshev weights were chosen according to a a side-lobe attenuation constraint of 50 dB. The DEDCs were calculated by evaluating the Schroeder integral in Eq. (6) up to the intersection time with the noise floor, cf. Method B in [17]. The DEDCs were truncated at the times corresponding to a level of 20 dB above the noise floor to compensate for errors introduced by limiting the integration interval [18]. The decay times $\langle T(\theta_q, \phi_q)\rangle$ were estimated from the respective DEDCs using linear regression in accordance with the T_{20} estimation specified in the international standard ISO-3382 [19]. A moving average filter with a time constant of approximately 4.2 ms was used to reduce influences of instantaneous energy fluctuations. All results presented in this paper were band pass filtered to the 500 Hz third-octave frequency band.

[2]For an analysis of the sound field isotropy during the decay based on the data, the reader is referred to [7, 13]

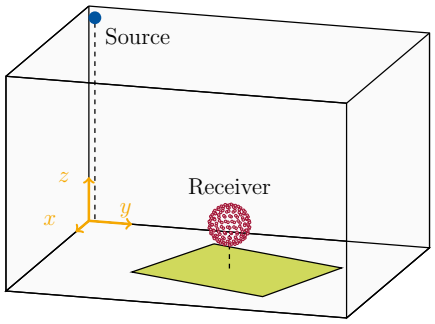

Figure 1: The experimental setup with source and receiver positions as well as the absorber position in the reverberation room. For better visual interpretability only sampling positions on the outer sphere are shown in.

Results

Figure 2 shows the normalized omnidirectional EDCs calculated from the omnidirectional response of the array for the two room configurations. For the room without panel diffusers one may clearly observe a bent in the EDC below −5 dB, clearly indicating a multi-exponential decay process governed by modes with unequal damping constants, as expected for a rectangular room without appropriate treatment [1, 4]. The addition of diffusers seemingly yields an approximately linear logarithmic EDC, indicating that the diffusers provide a fitting solution.
The estimated decay time constants $\langle T(\theta_q, \phi_q)\rangle$ for the directional mode groups are visualized in Fig. 3. All coordinate axes are aligned with the walls of the room, where the azimuth angles 0 ° and 90 ° define the positive x- and y-axes, respectively, cf. Fig. 1. Comparing the distributions for both room configurations it is observed that the room with diffuser panels shows a more uniform distribution over all angles. An exception is found at $(\theta, \phi) = (-55\,°, -100\,°)$, which is caused by large fluctuations in the DEDC for the respective direction. A

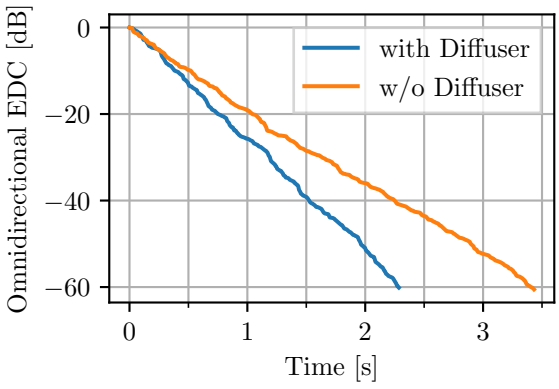

Figure 2: Normalized omnidirectional EDCs for the room with and without mounted panel diffusers.

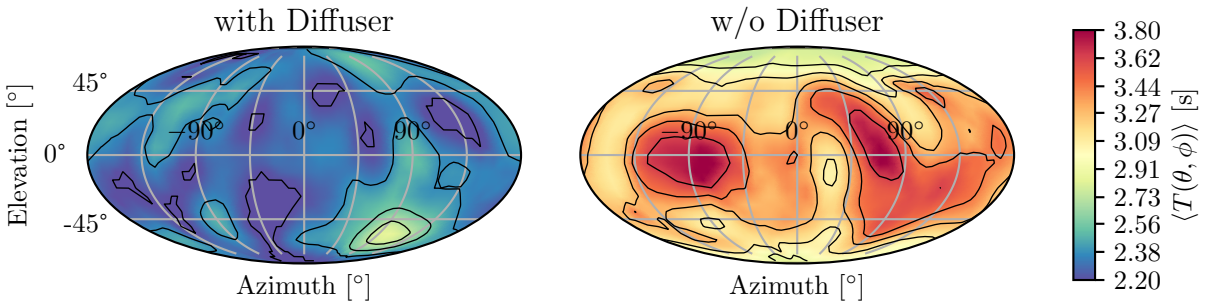

Figure 3: Directional distributions of decay constants estimated from the DEDC for the room occupied with an absorber sample and with and without panel diffusers. The coordinate system is aligned with the coordinate axes of the room. Azimuth angles 0 ° and 90 ° define the positive x- and y-axes, respectively, cf. Fig. 1. The grid lines represent steps of 45 °.

reason for the fluctuations is the amplitude of waves reflected from the absorber below the array which is small relative to waves with large amplitude leaking into the side-lobes of the beamformer.

The decay time distribution in the room without diffusers shows distinct maxima at $(\theta, \phi) = (0\,^\circ, \pm 90\,^\circ)$, which correspond to slowly decaying axial modes in the y-axis grazing to the absorber sample and therefore largely unaffected by it. In contrast, minima are found towards the poles corresponding to axial modes in the z-axis perpendicular to the absorber. Again, in the lower hemisphere, modes with larger energy – and typically larger decay times – leak into the side-lobes of the beamformer. This issue results in a flattening of the respective curve, inherently caused by groups of modes decaying at different rates, and hence in overestimating the decay time. Additionally, the distribution mostly shows a decrease in the decay times from the equator region towards the poles, hinting at separate groups of tangential modes with non-grazing incident onto the absorber sample towards the poles and grazing incidence in the xy-plane. Comparing Fig. 2 and Fig. 3 it is evident that without panel diffusers, the middle and late part of the EDC are clearly biased towards the decay times corresponding to the axial modes largely unaffected by the absorber sample, while shorter decay times corresponding to modes non-grazing to the absorber may only be visibly represented in the very early part of the EDC. These results seem to be in line with findings by Balint et al. [5] who found the decay in very similar experimental setup of a rectangular reverberation room to be governed by modes with two different decay constants using a Bayesian approach.

Conclusion

We presented an analysis of modes grouped according to their DOA in the two-dimensional wave number spectrum with regard their average decay times. The average decay times for the respective group were estimated from the DEDCs calculated from the wavenumber spectrum measured in a reverberation room equipped with and without panel diffusers. Results indicated angularly separable groups with systematic differences for the room without diffusers which can be attributed to the multi-exponential character of the omnidirectional EDC of the sound field in the room.

However, the results also showed issues caused by non-ideal separations of the mode groups due to insufficient side-lobe attenuation and angular resolution of the beamforming algorithm, which in turn resulted in DEDCs consisting of modes with different average damping constants, consequently showing multi-exponential characteristics. Application of an algorithm capable in extracting the decay constants of multi-exponential decay functions – such as presented by Balint et al. [5] is therefore expected to improve the results presented here while additionally providing angular information about the decay process.

Acknowledgements

The authors would like to thank Mélanie Nolan and Efren Fernandez-Grande for the collaboration and many fruitful discussions, and Samuel A. Verburg for his help with the experimental setup. Work presented here was funded under DFG Grant VO 600 41-1.

References

[1] F. V. Hunt, L. L. Beranek, and D. Y. Maa. “Analysis of Sound Decay in Rectangular Rooms”. In: *The Journal of the Acoustical Society of America* 11.1 (July 1939), pp. 80–94.

[2] M. Nolan, S. A. Verburg, J. Brunskog, and E. Fernandez-Grande. “Experimental Characterization of the Sound Field in a Reverberation Room”. In: *The Journal of the Acoustical Society of America* 145.4 (Apr. 2019), pp. 2237–2246.

[3] R. E. Halliwell. “Inter-laboratory Variability of Sound Absorption Measurement”. In: *The Journal of the Acoustical Society of America* 73.3 (Mar. 1983), pp. 880–886.

[4] E. Nilsson. “Decay Processes in Rooms with Non-Diffuse Sound Fields Part I: Ceiling Treatment with Absorbing Material”. In: *Building Acoustics* 11.1 (Mar. 1, 2004), pp. 39–60.

[5] J. Balint, F. Muralter, M. Nolan, and C.-H. Jeong. “Bayesian Decay Time Estimation in a Reverberation Chamber for Absorption Measurements”. In: *The Journal of the Acoustical Society of America* 146.3 (Sept. 2019), pp. 1641–1649.

[6] M. Berzborn and M. Vorländer. “Investigations on the Directional Energy Decay Curves in Reverber-

ation Rooms". In: *Proceedings of Euronoise*. Euronoise. Hersonissos, Crete, 2018, pp. 2005–2010.

[7] M. Berzborn, M. Nolan, E. Fernandez-Grande, and M. Vorländer. "On the Directional Properties of Energy Decay Curves". In: *Proceedings of the 23rd International Congress on Acoustics*. 2019, pp. 4043–4050.

[8] B. Rafaely, I. Balmages, and L. Eger. "High-Resolution Plane-Wave Decomposition in an Auditorium Using a Dual-Radius Scanning Spherical Microphone Array." In: *The Journal of the Acoustical Society of America* 122 (2007), pp. 2661–2668.

[9] B. Rafaely. "The Spherical-Shell Microphone Array". In: *IEEE Transactions on Audio, Speech and Language Processing* 16.4 (2008), pp. 740–747.

[10] B. Rafaely. *Fundamentals of Spherical Array Processing*. 1st Edition. Springer, 2015.

[11] E. G. Williams. *Fourier Acoustics*. Academic Press, 1999.

[12] M. R. Schroeder. "New Method of Measuring Reverberation Time". In: *The Journal of the Acoustical Society of America* 37.6 (1965), pp. 1187–1187.

[13] M. Nolan, M. Berzborn, and E. Fernandez-Grande. "Experimental Characterization of the Decaying Sound Field in a Reverberation Room". In: *Proceedings of the 23rd International Congress on Acoustics*. ICA. Aachen, Germany, 2019, pp. 4035–4042.

[14] P. Leopardi. "A Partition of the Unit Sphere into Regions of Equal Area and Small Diameter". In: *Electronic Transactions on Numerical Analysis* 25.12 (2006), pp. 309–327.

[15] G. Chardon, W. Kreuzer, and M. Noisternig. "Design of Spatial Microphone Arrays for Sound Field Interpolation". In: *IEEE Journal of Selected Topics in Signal Processing* 9.5 (2015), pp. 780–790.

[16] M. Berzborn, R. Bomhardt, J. Klein, J.-G. Richter, and M. Vorländer. "The ITA-Toolbox: An Open Source MATLAB Toolbox for Acoustic Measurements and Signal Processing". In: *Proceedings of the 43rd Annual German Congress on Acoustics*. DAGA. Kiel, 2017, pp. 222–225.

[17] M. Guski and M. Vorländer. "Comparison of Noise Compensation Methods for Room Acoustic Impulse Response Evaluations". In: *Acta Acustica united with Acustica* 100.2 (Mar. 1, 2014), pp. 320–327.

[18] A. Lundeby, T. E. Vigran, H. Bietz, and M. Vorl. "Uncertainties of Measurements in Room Acoustics". In: *Acta Acustica united with Acustica* 81.4 (July 1, 1995), pp. 344–355.

[19] International Organization for Standardization. *DIN EN ISO 3382: Acoustics - Measurement of Room Acoustic Parameters*. 2009.